Desalination and Water Treatment
www.deswater.com

doi:10.5004/dwt.2021.27251

226 (2021) 104–112
June

Removal of real multicomponent textile wastewater by adsorption onto graphene oxide nanoparticles: optimization of operating parameters

Elham Mohammadi Maroufi, Leila Amirkhani*, Hossein Zakaryazadeh

Department of Chemical Engineering, Ahar Branch, Islamic Azad University, 5451116714 Ahar, Iran, Tel. +98 4144239781; email: l-amirkhani@iau-ahar.ac.ir

Received 17 September 2020; Accepted 14 March 2021

ABSTRACT

In the present work, graphene oxide (GO) is synthesized successfully by the Hummer method. The product is characterized by various techniques such as scanning electron microscopy, Fourier transform infrared, X-ray diffraction, and UV-vis spectroscopy. The prepared GO is used as a novel absorbent to remove different dyes, organic, and inorganic pollutants from real textile wastewater. The effects of operational parameters like absorbent dosage (13–25 mg), pH (3–9), and contact time (12–30 min) on wastewater treatment are studied by response surface methodology. The optimized parameters are found to be 25 mg for GO dosage, pH 8, and 25 min for contact time. The chemical oxygen demand removal efficiency is calculated 62.10% under optimum conditions. These results suggest that the GO nanoparticles are a good candidate for the rapid remove of dyes and complicated pollutants from aqueous solutions.

Keywords: Adsorption; Graphene oxide; COD removal; RSM; Textile wastewater; Water purification

1. Introduction

Water is the one of the most important environmental resources on that living organisms and humans rely on to survive. Nowadays, the water source pollution by different organic and inorganic materials is becoming a serious concern [1]. The textile industry is one of the most important industries in the world. A lot of fresh water is consumed in the preparation, dyeing, rinsing, and other steps of this industry [2,3]. Textile wastewater due to a lot of dye auxiliaries and dyes are highly contaminated [4]. If these pollutants are discharged into the surrounding environment, they will produce high organic materials and results high toxicity and color [5,6]. In dyeing processes, about 15% of the total dyes enter the sewage and colored wastewater is produced in this way [7]. The textile industry mostly uses azo dyes, which are known as synthetic dyes [8]. The azo dyes are highly stable, and their structure is chemically resistant to external agents [9]. Several physical–chemical and biological techniques have been proposed over the past decades to wastewater treatment of the textile industry [10,11], but these techniques cannot degrade dyes and other pollutants completely. Biological treatments have some advantageous such as reasonable price and environmental compatibility. Unfortunately, the complete dye degradation is rarely reached by biological treatments and the toxic and carcinogenic aromatic amines can be formed during biological treatments of dyes [12,13], resulting in high chemical oxygen demand (COD). On the other hand, the physical-chemical techniques like adsorption are useful for decolorization and COD reduction. The adsorption technique is not destructive, because the pollutants are transferred from one phase to another and generate solid waste [14]. Activated carbon (AC) has been proposed as an excellent adsorbent for the remove of different inorganic and organic pollutants dissolved in water [15]. Activated carbon is the unprocessed form of graphite. The structure of activated carbon is different from graphite, because it has a random and irregular arrangement of atoms. Activated carbon has extremely porous structure and the pore size is different

* Corresponding author.

from molecular dimensions to visible cracks. Activated carbon has been used widely as an adsorbent due to its high chemical and mechanical stability, wonderful reactivity and excellent adsorption capacity [16]. Graphene oxide (GO) is also proposed as a very successful nano-adsorbent for the remove of pollutants like dyes. Impressive adsorption of industrial dyes such as malachite green, methyl orange, and BR-12 has been reported [17,18]. Li et al. have compared the adsorption results of methylene blue dye on GO and AC. They showed that the methylene blue adsorption on GO is stronger. Because the GO can interact with dyes via electrostatic interaction and π–π electron donor–acceptor interactions, but the interaction of AC is only based on the large surface area of AC [19]. It is reported that the GO has several advantages over the AC. Its characteristic structure and electronic property can result in strong interaction with organic molecules like industrial dyes, via non-covalent forces, such as van der Waals forces, π–π stacking, hydrogen bonding, electrostatic forces, and hydrophobic interactions. Its nano-sized structure also endows it some advantages like rapid equilibrium rates, high adsorption capacity, and effectiveness over a broad pH range [20]. Also, the adsorption capacity of graphene nanosheets and GO was studied for the removal of blue and red direct industrial textile dyes. The results indicated that GO provided a higher removal efficiency for both, blue and red colored dyes, due to the presence of their oxygen functional groups, which allow several types of electrostatic interactions and overcome the π–π stacking forces [21]. Different techniques have been proposed to synthesize GO powders. The chemical oxidation of graphite is the most preferred method based on Hummers method, because of its suitability for large-scale production [22]. Effect of processing conditions like different oxidant and their concentration were studied for GO synthesis and adsorption tests were performed with azo dyes as well as a kinetic study using real wastewater [23,24]. The operating parameters like pH, reaction time, initial pH, and absorbent dosage have significant effect on the GO performance. Recently, the effect of parameters to treat the real textile wastewater has been studied one by one, and the percentages removal of each textile wastewater sample have been investigated based on color and turbidity [25]. The effect of the parameters on each other has not been studied until now. According to our knowledge, there has been no paper published until now for the dye removal from real textile wastewater by GO nano-powders and studying the operation parameters based on response surface methodology (RSM). So, we have synthesized GO nano-powders and investigated their ability for wastewater treatment of a real textile industry. The novelty of this work is using of GO for textile wastewater treatment and optimization of operating parameters by the RSM based on central composite design (CCD). The reaction time, initial pH, and absorbent dosage have been studied as the experimental parameters.

2. Materials and methods

2.1. Graphene oxide synthesis

Graphene oxide was synthesized by Hummers method [22]. Graphite (10 g, Sinchem, SK 4206.0500, CAS. No: 7782-42-5, made in South Korea) and $NaNO_3$ (5 g, Merck, Darmstadt, Germany) were mixed with 240 mL of H_2SO_4 (95%–97%, Merck, Darmstadt, Germany) in a 1,000 mL flask. The suspension was stirred for 30 min at 0°C. Then, $KMnO_4$ (30 g, Merck, Darmstadt, Germany) was added carefully and the reaction temperature was controlled to keep lower than 20°C. Then, the suspension was stirred at room temperature overnight. 300 mL of H_2O was slowly added and the reaction temperature was increased up to 98°C. The suspension was stirred for 24 h and finally, 100 mL of H_2O_2 (30%, Merck, Darmstadt, Germany) was added to the mixture. The mixture was centrifuged with HCl and washed with deionized (DI) water. The solid was drying under vacuum and the graphene oxide (GO) was obtained as a gray powder.

2.2. Wastewater treatment

The real wastewater was taken from the carpet manufacturer in Tabriz, Iran. The wastewater was a complex combination comprising the residual dyes, benzene compounds, aromatic amines, and long-chain alkanes with an initial COD value of 2,568 mg L^{-1} and pH around 7.58. The adsorption treatments were applied on 200 mL of the textile wastewater by stirring on a shaker at 350 rpm for different GO dosage and time according to Table 3. Finally, the samples were centrifuged for 1 min at 3,000 rpm to separate the adsorbent prior to COD measurement. Emulsion blanks containing no adsorbent were also studied by the same experimental procedure. The characteristics of raw wastewater and the effect of centrifugation on un-treated and treated sample with GO are given in the Table 1. COD was measured according to the standard method specified in APHA [26].

2.3. Experimental design

In this study, GO dosage, contact time, and pH were introduced as RSM input variables. The experimental ranges of factors are shown in Table 2. The coded values were used for statistical calculations, based on the bellow equation [27]:

$$X_i = \frac{z_i - z_0}{\delta z} \quad (1)$$

where X_i indicates the coded level of the variable (dimensionless value), z_i, z_0, and δz denote the actual value of the variable, the center point of the variable and the interval variation, respectively. CCD is used to evaluate the direct interaction and quadratic relationship between the controllable input parameters. CCD with three input variables consists of 20 experiments with 8 cubic points (coded as ±1), 6 axial points (coded as ±2), and 6 replications of the central points of cubic to provide an estimation of the experimental error variance. Minitab 19 software is used for experiment design and data analysis. The design matrix of experiments is presented in Table 3.

3. Results and discussion

3.1. Physical characterization

The morphology of synthesized GO is investigated by SEM. Fig. 1a indicates the large surface areas of synthesized

Table 1
Characteristics of the raw real wastewater and the effect of centrifugation on un-treated and treated sample with GO

Parameter	Raw real wastewater	After centrifugation for un-treated sample	After centrifugation for treated sample with GO
pH	7.58	8	8
Temperature (°C)	30.0	25	25
Color (uH)	284.3	258.5	139.7
Turbidity (NTU)	112.1	99.2	48.2
BOD_5 (mg L^{-1})	2,181.7	1,938.2	171.8
COD (mg L^{-1})	2,568.0	2,316.3	973.5

Table 2
Experimental ranges and levels of the independent test variables

Variable	Ranges and levels				
	–2	–1	0	+1	+2
GO dosage (mg) (X_1)	13	15	19	23	25
pH (X_2)	3	4	6	8	9
Contact time (min) (X_3)	12	15	21	27	30

Table 3
3-factor central composite design matrix and the value of response function (COD: mg L^{-1})

Run	GO dosage (mg)	pH	Contact time (min)	COD (mg L^{-1})	
				Experimental	Predicted
1	0	0	0	1,382	1,458
2	0	0	0	1,402	1,458
3	+1	+1	–1	1,273	1,326
4	–1	+1	–1	1,611	1,725
5	+1	–1	–1	1,615	1,617
6	0	–2	0	1,652	1,649
7	–1	–1	–1	1,661	1,682
8	+1	+1	+1	1,108	1,146
9	0	0	0	1,434	1,458
10	0	0	0	1,475	1,458
11	+2	0	0	1,180	1,180
12	0	0	–2	1,784	1,682
13	–1	+1	+1	1,548	1,605
14	0	0	+2	1,531	1,526
15	0	+2	0	1,589	1,440
16	0	0	0	1,489	1,458
17	0	0	0	1,489	1,458
18	–1	–1	+1	1,647	1,653
19	+1	–1	+1	1,584	1,529
20	–2	0	0	1,680	1,573

GO by Hummer's method which has some 2-dimensional leaf-like flake feature. GO has a layered structure with some crumpling which is as a result of GO sheet scrolling.

Fig. 1b shows the XRD pattern of synthesized GO. The results show a sharp characteristic peak at 2θ = 11.61° with an interlayer distance of 6.78 A° and confirm the successful preparation of GO according to Zhang et al. [28]. The Fourier transform infrared (FTIR) spectra of GO is indicated in Fig. 2c.

The FTIR spectra of GO shows the intense absorption band at 3,410 cm^{-1}, related to bond stretching of O–H [19]. The peak at 1,625 cm^{-1} assigning to the characteristic bands of graphite structure (C=C) [29]. The peaks located at 1,738 and 1,418 cm^{-1} are attributed to the presence of C=O [30]. 1,245 and 1,061 cm^{-1} peaks are attributed to the C–O–C and C–O functional groups, respectively [31]. It is reported that the carboxyl and carbonyl groups are present at the edges of GO and the hydroxyl groups are located on the basal planes of GO [32]. The FTIR results show that the synthesized GO has oxygen-containing functional groups. These functional groups gives some chemical adsorption sites for interaction with pollutants. The textural characteristics of GO are studied by N_2-BET surface area analysis. The specific surface area, pore volume, and average pore diameter of GO is observed 153.64 m^2 g^{-1}, 0.093 cm^3 g^{-1}, and 2.58 nm, respectively. The physical adsorption capacity of an adsorbent depends mainly on the surface area. As observed by N_2-BET surface area results, the surface area of GO is high enough to interact with dyes and pollutants. Optical absorption property of GO was determined by UV-vis spectroscopy and shown in Fig. 1d. Absorption spectra of aqueous dispersion of GO showed a sharp peak at ~230 nm corresponding to π–π* transition of aromatic C=C bonds and a shoulder peak at ~295 nm attributed to *n*–π* transition of carbonyl groups. The appearance of π–π* peak shows that the synthesized GO is highly oxidized and contains mainly mono- or bi-layers GO. The result clearly indicated the presence of unsaturated carbon ring and oxygen containing functional groups within the structure [33]. This observation was analogous to that of FTIR (Fig. 1c) results.

3.2. CCD model and residuals analysis

A second-order (quadratic) polynomial response surface model (Eq. (2)) is used to the experimental result fit obtained by CCD. This model describes a polynomial approximation of experimental results with the following relationship:

$$Y = b_0 + \sum_{i=1}^{n}\left(b_i X_i\right) + \sum_{i=1}^{n}\left(b_{ii} X_{ii}^2\right) + \sum\nolimits_{ij=1}^{n}\left(b_{ij} X_i X_j\right) \quad (2)$$

where Y denotes the predicted response, X_i is the coded experimental levels of the variable, b_0 indicates a constant

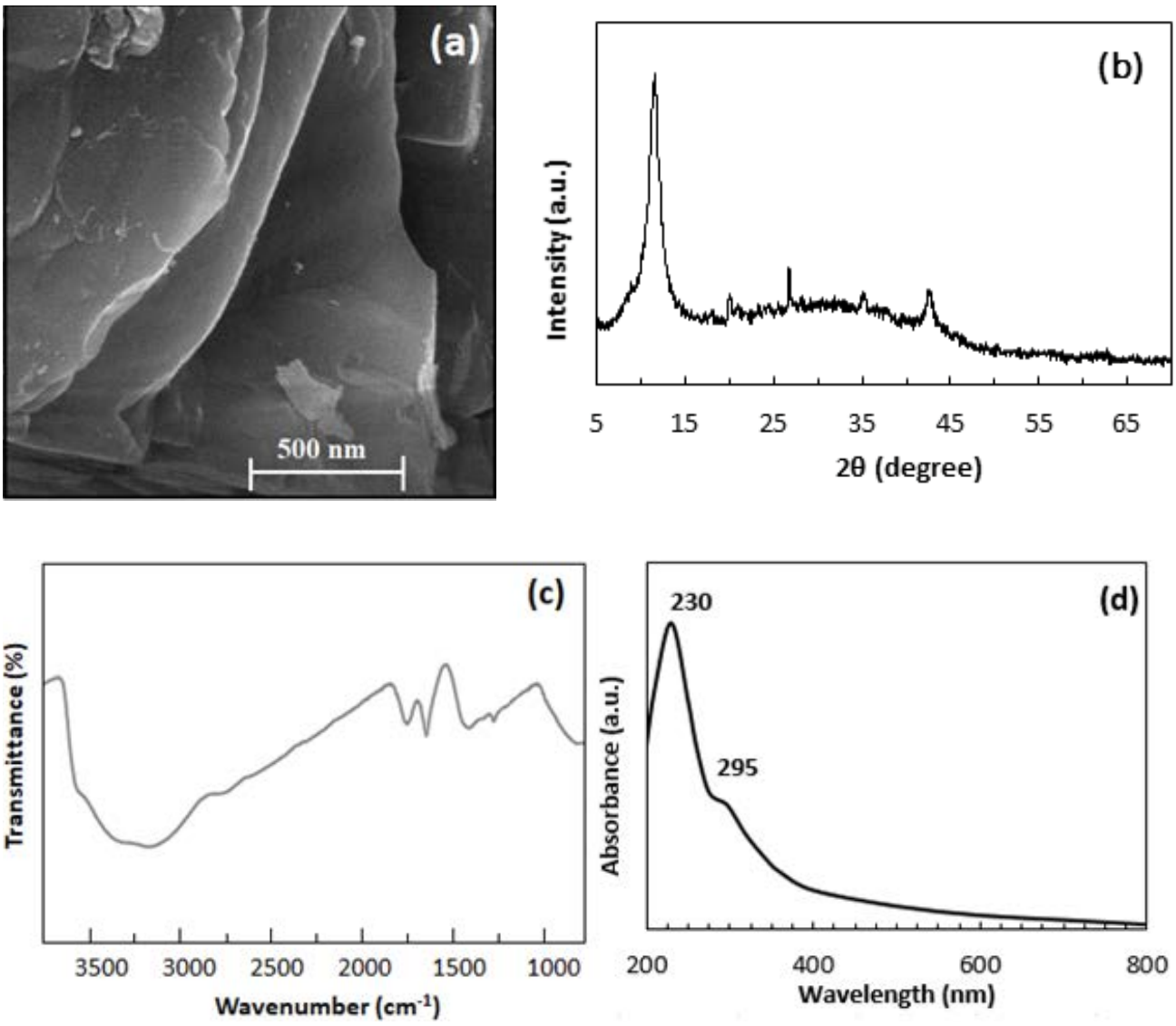

Fig. 1. SEM image (a), XRD pattern (b), FTIR spectra (c) of synthesized GO, and (d) UV-vis spectrum of aqueous dispersion of GO.

and b_i, b_{ii}, and b_{ij} show the regression coefficients for the linear, quadratic and interaction effects, respectively [27,34]:

Based on these results, the empirical relationship between the response and independent variables is expressed as follows:

$$Y = 1,255 + 128.9x_1 + 51x_2 - 61.2x_3 - 2.26x_1^2 + 12.12x_2^2 + 1.804x_3^2 - 10.45x_1x_2 - 0.62x_1x_3 - 1.91x_2x_3 \quad (3)$$

The COD values of real textile wastewater after treatment by GO adsorption technique are predicted by Eq. (3) and presented in Table 3. These results show the good agreements between the experimental and predicted values of COD values. The significance and adequacy of the model are evaluated by analysis of variance (ANOVA) and the obtained results are shown in Table 4.

The correlation between the experimental data and the predicted responses is evaluated quantitatively by the correlation coefficient (R^2). The results show that the predicted values matched the experimental values reasonably well with R^2 = 0.8551. It means that 85.51% of the variations in COD are explained by the proposed model and only 14.49% of variations cannot be explained by the model. Adjusted R^2 (Adj-R^2) is also a measure of the goodness of a fit and it is more suitable for comparing models with different numbers of independent variables. If there are many terms in a model and not very large sample size, Adj-R^2 may be visibly smaller than R^2 [35]. The value of Adj-R^2 is found 0.7247, which is very close to the corresponding R^2 value.

In addition to the criteria for assessing the adequacy of the models mentioned above, the difference between the predicted and experimental responses (residuals) are often measured to investigate the adequacy of the model. The residuals are considered as elements of variation unexplained by the fitted model and they occur based on a

Table 4
Analysis of variance (ANOVA) for the fit of COD values from central composite design

Source	DF[a]	SS[b]	Adj-MS[c]	*F*-value	*P*-value
Regression	9	481,363	53,485	6.56	0.003
Residual error	10	81,561	8,156	–	–
Lack-of-fit	5	70,850	14,170	2.61	0.059
Pure error	10	81,561	8,156	–	–
Total	19	562,924	–	–	–

[a]Degree of freedom.
[b]Sum of squares.
[c]Adjusted mean square.

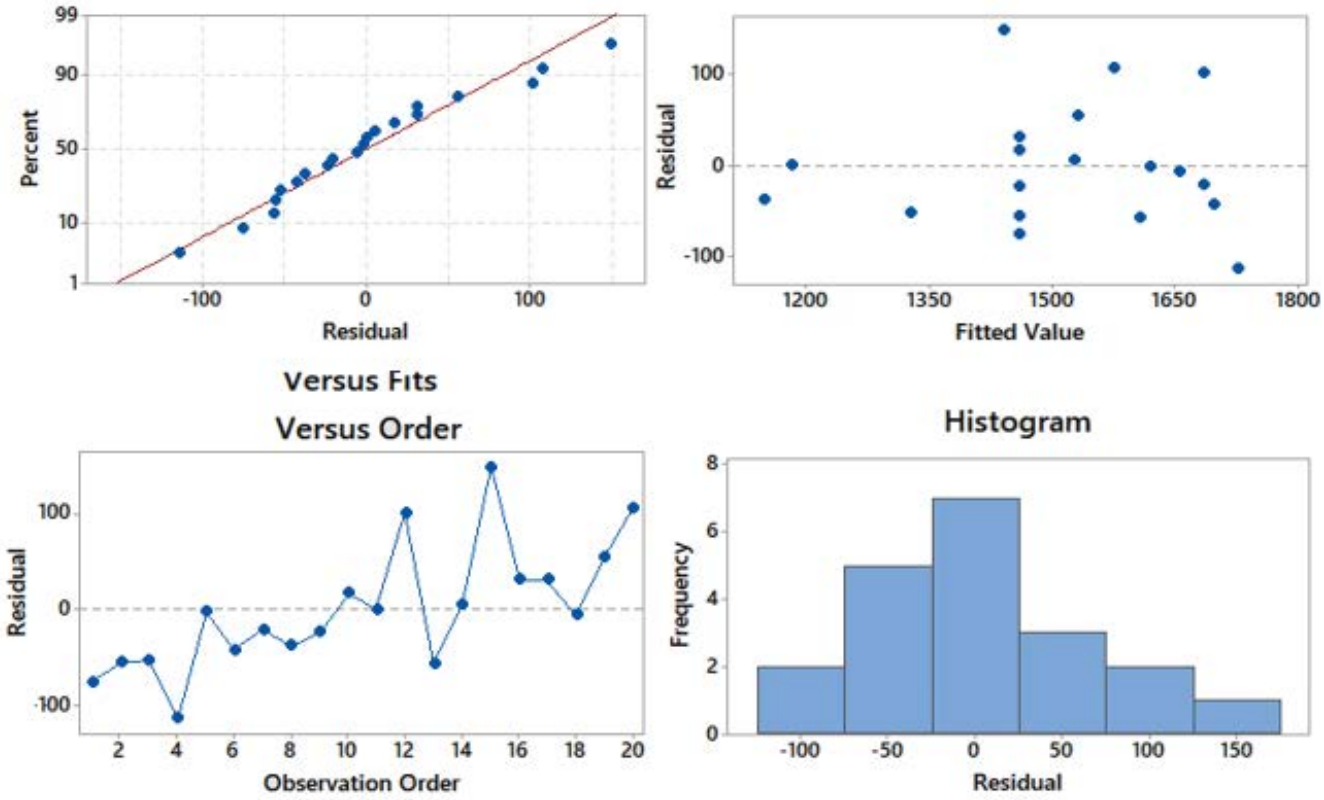

Fig. 2. Residual plots for COD values of textile wastewater treatment by GO.

normal distribution, if the model will be a good predictor [36]. Four residual plots are provided by Minitab software for investigation of the residual normal distribution.

The normal probability plots of residuals and residuals vs. fit plots are shown in Fig. 2. Trends observed in Fig. 2 indicate reasonably well-behaved residuals. According to these plots, the residuals are randomly scattered. The total variation of the results is subdivided into two components by ANOVA: variation associated with the experimental error and variation associated with the model [37].

F-value is calculated by diving the mean square of the model to the residual error. *F*-value will be greater than the tabulated value, if the model is a good predictor for experimental results. Here, *F*-value is obtained 6.56, which is greater than the tabulated *F* (2.352 at the 95% significance). It means that the adequacy of the model fits is confirmed.

3.3. Determination of importance of model terms

The Student's *t* distribution and the corresponding values, along with the parameter estimate, are given in Table 5 to determine the effective terms of the developed model. The greater *T*-value and the smaller *P*-value (less than 0.05 at the 95% significance) for a coefficient indicate the most significant influence of it [38].

The coefficients with *P*-value greater than 0.05 are eliminated and Eq. (3) is rewritten as follows:

$$Y = 1,255 + 128.9x_1 + 518x_2 + 1.804x_3^2 - 10.45x_1x_2 \quad (4)$$

Table 5
T and *P* values for the proposed model parameters

Parameter	*T*-value	*P*-value
b_0	40.42	0.000
b_1	–5.13	0.000
b_2	–3.32	0.008
b_3	–2.04	0.068
b_1b_1	–1.29	0.227
b_2b_2	1.72	0.115
b_3b_3	2.31	0.044
b_1b_2	–2.62	0.026
b_1b_3	–0.47	0.651
b_2b_3	–0.72	0.490

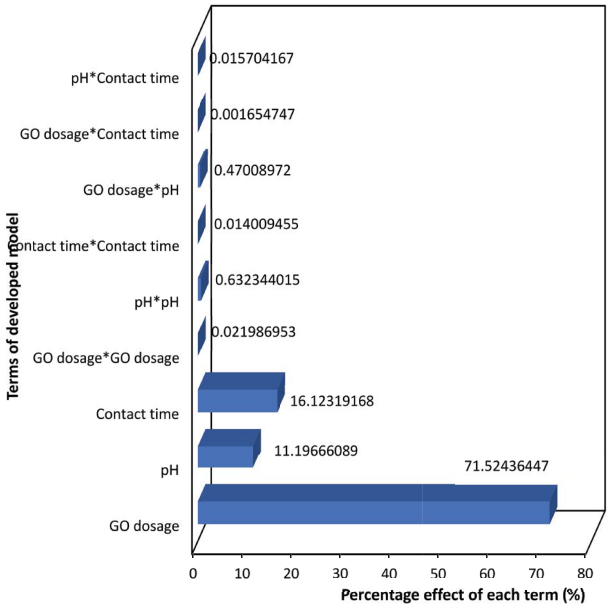

Fig. 3. Pareto graphic analysis of COD values.

Also, the Pareto analysis can be applied to determine the significance of each factor. According to this analysis the percentage effect of each factor (P_i) on the response can be calculated as:

$$P_i = \left(\frac{b_i^2}{\sum_{i=1}^{n} b_i^2} \right) \times 100 \qquad i \neq 0 \qquad (5)$$

The Pareto graphic analysis is shown in Fig. 3. The results indicate that among the variables, GO dosage (71.52%), contact time (16.12%), and pH (11.20%) produce the highest effect on COD value.

3.4. Effects of variables on the COD of wastewater

As concluded above, the GO dosage, contact time, and pH are the most important factors in COD values of wastewater. Fig. 4 illustrates 2-dimensional counter plot and 3-dimensional response surface for investigating the interactions between the variables. The *X* and *Y*-axis values of these figures are the real values. The most important parameter to be considered is the effect of adsorbent dosage, because the extent of de-colorization is specified by it and the GO dosage will predict the cost of adsorbent per unit of the solution to be treated. Figs. 4a and c demonstrate that the COD value is decreased sharply by increasing the GO dosage and the trend of COD decrease is very close to be linear [39]. The degree of COD decrease with the adsorbent dosage commonly depends on the adsorption site availability and the surface area at a fixed dye concentration. More adsorption sites result in a higher amount of dye and other pollutant removal. The effect of contact time is shown in Figs. 4a and

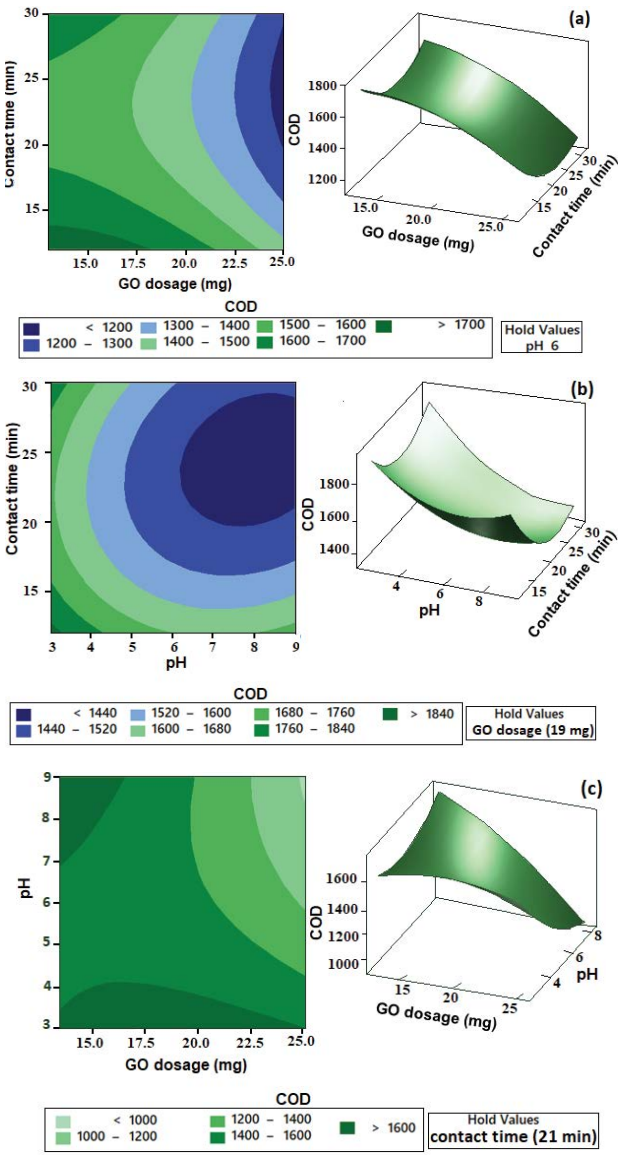

Fig. 4. Response surface and counterplots of COD values as a function of (a) GO dosage (mg) and contact time (min), (b) pH and contact time (min), and (c) GO dosage (mg) and pH.

b, the results indicate that the COD is decreased by increasing the contact time and the minimum COD is achieved at 25 min. By increasing the contact time up to 30 min, the COD value is almost as same as 25 min. Generally, by prolonging the contact time, the amount of absorbed dye, and removal efficiency will be increased [39]. At first, the amount of dye adsorbed onto the GO surface increases quickly, and later the process slows down and reaches a steady level [40]. At this step, the amount of the dye being adsorbed onto the GO is in a dynamic equilibrium with the amount of the dye desorbing from the GO and this time is named as equilibrium time [41]. This case is related to a decrease in prompt solute adsorption because of the absence of accessible open sites for dye adsorption (saturation) [42]. The amount of dye adsorbed at the equilibrium time shows the maximum adsorption capacity of the adsorbent under diffusion phenomenon [43]. Effect of solution pH is indicated in Figs. 4b and c. When pH of the textile wastewater solutions was increased from 3 to 6, the amounts of COD is decreased. On further increase in pH from 6 to 9, the amount of COD is increased. It means that the adsorption of dyes and pollutants is increased with pH up to 6 (Fig. 4b) and then slightly declined with a further increase in pHs. Most of the dyes used in the textile industry are characterized by azo bonds (N=N) having $–SO_3$, $–COO^-$, and OH^- groups. In other words, azo dyes are easily dissolved in water, so they are not prone to be flocculated [44]. It is demonstrated that the adsorption of dyes is strongly related to the zero-point charge (zpc) of adsorbent, isoelectric point (IEP) of dyes and solution pH. The pH_{zpc} of GO is found 6.5 by using a zeta potential meter. The surface charge of GO will be positive below pH 6.5 and negative above pH 6.5. The IEP of different azo dyes is reported at pH 6.8–7 [45]. So, at the pH above 6.8–7, the net charge of dyes becomes negative. The negatively charged sites of the GO does not prefer to adsorb the negatively charged dyes because of the electrostatic repulsion. On the other side, at lower pHs, the powerful electrostatic repulsion is between the positively charged sites of the GO ($pH_{zpc,GO}$ = 6.5) and dye cations (pH_{iep} = 6.8–7). So, the adsorption capacity of GO is decreased and the COD values are increased in the acidic range of pHs, especially when the pH was lower than 6. The negatively charged sites of the GO and the positively charged dyes is significantly attracted each other by electrostatic force for pHs in the range of 6.0–7.0. The adsorption capacity of dyes is increased with pHs up to ≈6.5 (Fig. 4) and then slightly decreased with the further increase in pHs.

3.5. Determination of optimal conditions for cell voltage

The quadratic models obtained by the RSM can be used to optimize and minimize the COD. To confirm the reliability of the model established in this study, the validation

Table 6
Comparison between previous works and the present one

Wastewater	Adsorbent	Conditions	Removal	Ref.
Textile wastewater	GO	pH = 5.8 *t*: 30 min Adsorbent dose: 0.8 g L^{-1} Initial COD: 715.4 mg L^{-1}	60.0% color	[23]
Textile wastewater	GO	pH = 6 *t*: 30 min Adsorbent dose: 0.46 g L^{-1} Initial COD: 715.4 mg L^{-1}	60.9% COD	[25]
Textile wastewater	Coal fly ash	pH ≤ 2 *t*: 3–5 min Adsorbent dose: 12–40 g L^{-1} *T*: 20°C–25°C Initial COD: 665 mg L^{-1}	44.44%–61.11% COD	[46]
Textile wastewater	Natural material	pH = 2–12 *t*: 90–160 min Adsorbent dose: 1.5 g L^{-1} *T*: room temperature Initial COD: 440 mg L^{-1}	M1: 88% COD M2: 79% COD	[47]
Cotton textile wastewater	Activated carbon from bamboo	Adsorbent dose: 3 g L^{-1} Initial COD: 251.65 mg L^{-1} *T*: 30°C	73.98% COD	[48]
Textile wastewater	GO	pH = 8 Adsorbent dose: 0.125 g L^{-1} *T*: room temperature *t*: 25 min Initial COD: 2,568 mg L^{-1}	62.1% COD	Present work

experiments are performed three times under the operating conditions predicted by the model for minimum COD. The optimum values of the process variables for the minimum COD are 25 mg for GO dosage (X_1), pH = 8 (X_2) and 25 min for contact time (X_3). At these optimum conditions, the predicted and observed COD are 983 and 982, 965 mg L^{-1}, respectively. It implies that the strategy to optimize the textile wastewater treatment and COD removal by RSM is successful. The initial value of COD before wastewater treatment by the adsorption technique was 2,568 mg L^{-1}. The COD removal efficiency was calculated 62.10% by Eq. (6):

$$\text{Removal efficency} = \frac{\left[\text{COD}_i\right] - \left[\text{COD}_f\right]}{\left[\text{COD}_i\right]} \times 100 \quad (6)$$

where $[COD_i]$ and $[COD_f]$ correspond to the COD value of textile wastewater at the initial and final path of treatment, respectively.

3.6. Performance comparison with literature

In Table 6, there is a comparison between several related previous reports. As shown in this Table 6, the present work with low adsorbent dose in high initial COD concentration, we have reached an important COD removal percentage in short time. Thus, GO nanoparticles could be a promising adsorbent for real textile treatment.

4. Conclusion

The GO is synthesized by Hummer method and used as an adsorbent for dye removal from real textile wastewater. The effect of operating parameters including GO dosage (13–25 mg) (g), wastewater pH (3–9) and contact time (12–30 min) of GO with wastewater on the COD of textile wastewater is studied by RSM. A good coefficient of determination (R^2 = 0.8551 and Adj-R^2 = 0.7247) between experimental and predicted COD values is achieved. The minimum value of COD is obtained by CCD under optimum conditions (25 mg for GO dosage, pH = 8, and 25 min for contact time). The COD removal efficiency of the proposed technique is calculated 62.10% under optimum conditions. Conclusively, the applying of adsorption technique by GO with other methods like biological treatments can be introduced as a powerful tool and potentially viable technique to the superior improvement of dye pollution control and wastewater treatment.

References

[1] S.-J. Park, T.-I. Yoon, J.-H. Bae, H.-J. Seo, H.-J. Park, Biological treatment of wastewater containing dimethyl sulphoxide from the semi-conductor industry, Process Biochem., 36 (2001) 579–589.

[2] C.R. Holkar, A.J. Jadhav, D.V. Pinjari, N.M. Mahamuni, A.B. Pandit, A critical review on textile wastewater treatments: possible approaches, J. Environ. Manage., 182 (2016) 351–366.

[3] G.K. Parshetti, A.A. Telke, D.C. Kalyani, S.P. Govindwar, Decolorization and detoxification of sulfonated azo dye methyl orange by *Kocuria rosea* MTCC 1532, J. Hazard. Mater., 176 (2010) 503–509.

[4] S. Benkhaya, S. M'rabet, A. El Harfi, A review on classifications, recent synthesis and applications of textile dyes, Inorg. Chem. Commun., 115 (2020) 107891 , 35 pages, doi: 10.1016/j.inoche.2020.107891.

[5] D.A. Yaseen, M. Scholz, Textile dye wastewater characteristics and constituents of synthetic effluents: a critical review, Int. J. Environ. Sci. Technol., 16 (2019) 1193–1226.

[6] C. Zhao, H. Zheng, Y. Sun, S. Zhang, J. Liang, Y. Liu, Y. An, Evaluation of a novel dextran-based flocculant on treatment of dye wastewater: effect of kaolin particles, Sci. Total Environ., 640–641 (2018) 243–254.

[7] B. Merzouk, B. Gourich, A. Sekki, K. Madani, C. Vial, M. Barkaoui, Studies on the decolorization of textile dye wastewater by continuous electrocoagulation process, Chem. Eng. J., 149 (2009) 207–214.

[8] I.M. Banat, P. Nigam, D. Singh, R. Marchant, Microbial decolorization of textile-dye containing effluents: a review, Bioresour. Technol., 58 (1996) 217–227.

[9] M.B. Ceretta, I. Durruty, A.M.F. Orozco, J.F. González, E.A. Wolski, Biodegradation of textile wastewater: enhancement of biodegradability via the addition of co-substrates followed by phytotoxicity analysis of the effluent, Water Sci. Technol., 2017 (2018) 516–526.

[10] I.M.C. Gonçalves, A. Gomes, R. Brás, M.I.A. Ferra, M.T.P. Amorim, R.S. Porter, Biological treatment of effluent containing textile dyes, Color. Technol., 116 (2000) 393–397.

[11] R.G. Saratale, G.D. Saratale, J.S. Chang, S.P. Govindwar, Bacterial decolorization and degradation of azo dyes: a review, J. Taiwan Inst. Chem. Eng., 42 (2011) 138–157.

[12] M. Işık, D.T. Sponza, Monitoring of toxicity and intermediates of C.I. Direct Black 38 azo dye through decolorization in an anaerobic/aerobic sequential reactor system, J. Hazard. Mater., 114 (2004) 29–39.

[13] Č. Novotný, N. Dias, A. Kapanen, K. Malachová, M. Vándrovcová, M. Itävaara, N. Lima, Comparative use of bacterial, algal and protozoan tests to study toxicity of azo- and anthraquinone dyes, Chemosphere, 63 (2006) 1436–1442.

[14] H. Hayat, Q. Mahmood, A. Pervez, Z.A. Bhatti, S.A. Baig, Comparative decolorization of dyes in textile wastewater using biological and chemical treatment, Sep. Purif. Technol., 154 (2015) 149–153.

[15] K. Karthick, C. Namasivayam, L.A. Pragasan, Kinetics and isotherm studies on acid dye adsorption using thermal and chemical activated Jatropha husk carbons, Environ. Prog. Sustainable Energy, 37 (2018) 719–732.

[16] R. Malik, D.S. Ramteke, S.R. Wate, Adsorption of malachite green on groundnut shell waste based powdered activated carbon, Waste Manage., 27 (2007) 1129–1138.

[17] D. Robati, B. Mirza, M. Rajabi, O. Moradi, I. Tyagi, S. Agarwal, V.K. Gupta, Removal of hazardous dyes-BR 12 and methyl orange using graphene oxide as an adsorbent from aqueous phase, Chem. Eng. J., 284 (2016) 687–697.

[18] D. Robati, M. Rajabi, O. Moradi, F. Najafi, I. Tyagi, S. Agarwal, V.K. Gupta, Kinetics and thermodynamics of malachite green dye adsorption from aqueous solutions on graphene oxide and reduced graphene oxide, J. Mol. Liq., 214 (2016) 259–263.

[19] Y. Li, Q. Du, T. Liu, X. Peng, J. Wang, J. Sun, Y. Wang, S. Wu, Z. Wang, Y. Xia, L. Xia, Comparative study of methylene blue dye adsorption onto activated carbon, graphene oxide, and carbon nanotubes, Chem. Eng. Res. Des., 91 (2013) 361–368.

[20] M.S. Mauter, M. Elimelech, Environmental applications of carbon-based nanomaterials, Environ. Sci. Technol., 42 (2008) 5843–5859.

[21] L.K. de Assis, B.S. Damasceno, M.N. Carvalho, E.H.C. Oliveira, M.G. Ghislandi, Adsorption capacity comparison between graphene oxide and graphene nanoplatelets for the removal of coloured textile dyes from wastewater, Environ. Technol., 41 (2020) 2360–2371.

[22] W.S. Hummers, R.E. Offeman, Preparation of graphitic oxide, J. Am. Chem. Soc., 80 (1958) 1339.

[23] C.M.B. de Araujo, G.F.O. do Nascimento, G.R.B. da Costa, K.S. da Silva, A.M. Salgueiro Baptisttella, M.G. Ghislandi, M.A. da Motta Sobrinho, Adsorptive removal of dye from

real textile wastewater using graphene oxide produced via modifications of hummers method, Chem. Eng. Commun., 206 (2019) 1375–1387.
[24] G.F.O. do Nascimento, G.R.B. da Costa, C.M.B. de Araújo, M.G. Ghislandi, M.A. da Motta Sobrinho Graphene-based materials production and application in textile wastewater treatment: color removal and phytotoxicity using *Lactuca sativa* as bioindicator, J. Environ. Sci. Health., Part A, 55 (2020) 97–106.
[25] C.M.B. de Araújo, G.F.O. do Nascimento, G.R.B. da Costa, A.M.S. Baptisttella, T.J.M. Fraga, R.B. de Assis Filho, M.G. Ghislandi, M.A. da Motta Sobrinho, Real textile wastewater treatment using nano graphene-based materials: optimum pH, dosage, and kinetics for colour and turbidity removal, Can. J. Chem. Eng., 98 (2020) 1429–1440.
[26] APHA, AWWA, WEF, Standard Methods for the Examination of Water and Wastewater, American Public Health Association, American Water Works Association, Water Environment Federation, Washington, DC, 1998.
[27] M. Poroch-Seritan, S. Gutt, G. Gutt, I. Cretescu, C. Cojocaru, T. Severin, Design of experiments for statistical modeling and multi-response optimization of nickel electroplating process, Chem. Eng. Res. Des., 89 (2011) 136–147.
[28] B.-T. Zhang, H.-F. Li, X. Zheng, Y. Teng, Y. Liu, J.-M. Lin, Preparation of durable graphene-bonded titanium fibers for efficient microextraction of phthalates from aqueous matrices and analysis with gas chromatography–mass spectrometry, J. Chromatogr. A, 1370 (2014) 9–16.
[29] P. Wu, Y. Qian, P. Du, H. Zhang, C. Cai, Facile synthesis of nitrogen-doped graphene for measuring the releasing process of hydrogen peroxide from living cells, J. Mater. Chem., 22 (2012) 6402–6412.
[30] A. Pulido, P. Concepción, M. Boronat, C. Botas, P. Alvarez, R. Menendez, A. Corma, Reconstruction of the carbon sp^2 network in graphene oxide by low-temperature reaction with CO, J. Mater. Chem., 22 (2012) 51–56.
[31] S. Chandra, P. Das, S. Bag, R. Bhar, P. Pramanik, Mn_2O_3 decorated graphene nanosheet: an advanced material for the photocatalytic degradation of organic dyes, Mater. Sci. Eng., B, 177 (2012) 855–861.
[32] M. Fang, K. Wang, H. Lu, Y. Yang, S. Nutt, Covalent polymer functionalization of graphene nanosheets and mechanical properties of composites, J. Mater. Chem., 19 (2009) 7098–7105.
[33] M. Yosef, A. Fahmy, W. El Hotaby, A.M. Hassan, A.S.G. Khalil, B. Anis, High performance graphene-based PVF foam for lead removal from water, J. Mater. Res. Technol., 9 (2020) 11861–11875.
[34] M. Zarei, A. Niaei, D. Salari, A. Khataee, Application of response surface methodology for optimization of peroxi-coagulation of textile dye solution using carbon nanotube–PTFE cathode, J. Hazard. Mater., 173 (2010) 544–551.
[35] S.C.R. Santos, R.A.R. Boaventura, Adsorption modelling of textile dyes by sepiolite, Appl. Clay Sci., 42 (2008) 137–145.
[36] L.A. Sarabia, M.C. Ortiz, Chapter 1.12 – Response Surface Methodology A2, S.D. Brown, R. Tauler, B. Walczak, Eds., Comprehensive Chemometrics, Elsevier, Oxford, 2009, pp. 345–390.
[37] E. Ghiasi, A. Malekzadeh, Removal of various textile dyes using $LaMn(Fe)O_3$ and $LaFeMn_{0.5}O_3$ nanoperovskites; RSM optimization, isotherms and kinetics studies, J. Inorg. Organomet. Polym. Mater., 30 (2020) 2789–2804.
[38] J.A. Cornell, Response Surfaces: Designs and Analyses, Marcel Dekker, Inc., New York, NY, 1987.
[39] A. Bhatnagar, A.K. Jain, A comparative adsorption study with different industrial wastes as adsorbents for the removal of cationic dyes from water, J. Colloid Interface Sci., 281 (2005) 49–55.
[40] B.H. Hameed, A.T.M. Din, A.L. Ahmad, Adsorption of methylene blue onto bamboo-based activated carbon: kinetics and equilibrium studies, J. Hazard. Mater., 141 (2007) 819–825.
[41] G. Atun, G. Hisarli, W.S. Sheldrick, M. Muhler, Adsorptive removal of methylene blue from colored effluents on fuller's earth, J. Colloid Interface Sci., 261 (2003) 32–39.
[42] N. Graham, X.G. Chen, S. Jayaseelan, The potential application of activated carbon from sewage sludge to organic dyes removal, Water Sci. Technol., 43 (2001) 245–252.
[43] I.A.W. Tan, A.L. Ahmad, B.H. Hameed, Adsorption of basic dye using activated carbon prepared from oil palm shell: batch and fixed bed studies, Desalination, 225 (2008) 13–28.
[44] V.K. Gupta, I. Ali, V.K. Saini, Adsorption studies on the removal of Vertigo Blue 49 and Orange DNA13 from aqueous solutions using carbon slurry developed from a waste material, J. Colloid Interface Sci., 315 (2007) 87–93.
[45] T.-H. Kim, C. Park, E.-B. Shin, S. Kim, Decolorization of disperse and reactive dye solutions using ferric chloride, Desalination, 161 (2004) 49–58.
[46] C. Zaharia, D. Suteu, Coal fly ash as adsorptive material for treatment of a real textile effluent: operating parameters and treatment efficiency, Environ. Sci. Pollut. Res., 20 (2013) 2226–2235.
[47] O. Assila, K. Tanji, M. Zouheir, A. Arrahli, L. Nahali, F. Zerrouq, A. Kherbeche, Adsorption studies on the removal of textile effluent over two natural eco-friendly adsorbents, J. Chem., 2020 (2020) 6457825, 13 pages, doi: 10.1155/2020/6457825.
[48] A.A. Ahmad, B.H. Hameed, Effect of preparation conditions of activated carbon from bamboo waste for real textile wastewater, J. Hazard. Mater., 173 (2010) 487–493.